

Journal of Biomedical Optics

SPIEDigitalLibrary.org/jbo

Cellular viscoelasticity probed by active rheology in optical tweezers

Evgeny V. Lyubin
Maria D. Khokhlova
Maria N. Skryabina
Andrey A. Fedyanin

Cellular viscoelasticity probed by active rheology in optical tweezers

Evgeny V. Lyubin, Maria D. Khokhlova, Maria N. Skryabina, and Andrey A. Fedyanin

Lomonosov Moscow State University, Faculty of Physics, 119991 Moscow, Russia

Abstract. A novel approach to probe viscoelastic properties of cells based on double trap optical tweezers is reported. Frequency dependence of the tangent of phase difference in the movement of the opposite erythrocyte edges while one of the edges is forced to oscillate by optical tweezers appeared to be highly dependent on the rigidity of the cellular membrane. Effective viscoelastic parameters characterizing red blood cells with different stiffnesses (normal and glutaraldehyde-fixed) are determined. It is shown that the photo-induced effects caused by laser trapping at the power level used in the experiments are negligible giving the possibility to use the offered technique for dynamic monitoring of soft materials viscoelastic properties. © 2012 Society of Photo-Optical Instrumentation Engineers (SPIE). [DOI: 10.1117/1.JBO.17.10.101510]

Keywords: optical tweezers; red blood cells; viscoelastic properties; active cell rheology.

Paper 12123SS received Feb. 21, 2012; revised manuscript received Apr. 12, 2012; accepted for publication Apr. 23, 2012; published online Jun. 8, 2012.

1 Introduction

Various techniques for local viscoelastic properties and deformability of complex materials research ranging from investigation of complex fluids to soft solids are of great practical and fundamental importance. In particular, viscoelastic characterization of cellular membranes is a crucial problem in understanding of tissue physiology. Methods probing the membrane viscoelastic properties provide tools to characterize the physiological state of the membrane and its changes caused by various diseases or drug effects. The most mainstay techniques which allow working with single cells are optical tweezers,¹⁻⁴ micropipette aspiration technique,⁵⁻⁷ and atomic force microscopy.^{8,9} Some of these methods are based on the analysis of the studied system behavior under external periodic perturbation. Recently a new method to study viscoelasticity of the red blood cell (RBC) membrane was proposed¹⁰ by attaching a functionalized ferromagnetic microbead to the RBC membrane and exposing the system in the ac-magnetic field. The magnetic bead's motion caused the deformation of the membrane and elastic and frictional moduli were extracted from optically tracked bead motion. However the only method having the ability for ultra-fine positioning, control and noninvasive probing of local object properties in aqueous solution having no impact from the bulk substrate is the optical tweezers technique which is a unique tool for exploring problems related to quantitative characterization of single objects at the microscale.¹¹⁻¹³ This method is widely used to determine the elastic properties of cell membranes, in particular the RBC membranes.^{14,15} Here we report on a new way to employ optical tweezers to dynamically probe viscoelastic properties of the cells. We use so-called active rheology meaning that the motion of the studied objects is analyzed on the frequencies of external perturbations caused by optical traps. This approach is the further development of so-called passive rheology¹⁶ monitoring the thermal fluctuations to

measure the effect of hydrodynamic coupling on the dynamics of two colloidal particles held in fixed optical traps.¹⁷

In the present work active rheology is combined with an analysis of forced RBC vibration when the cell is optically trapped in double optical tweezers. This approach allows marking out correlated displacements of trapped erythrocyte edges. The displacements determined using forced vibrations analysis in the frequency range up to 1 kHz quantitatively characterize the viscoelastic properties of individual RBC. A new dynamic parameter, namely, the tangent of phase difference in the movement of the erythrocyte edges, is introduced as an effective fingerprint characterizing the state of the cell.

2 Materials and Methods

Fresh blood was taken from donors by a fingertip needle prick. For sample preparation 0.2 μl of blood was suspended in 1 ml of autologous plasma, which was previously obtained by whole venous blood centrifugation (first 3500 RPM, 25°C, 7 min, then 20,000 RPM, 25°C, 7 min). Centrifugation was carried out in order to purify plasma from formed elements of the blood including platelets that can be trapped together with RBCs preventing correct measurements. Then 40 μl of the RBC suspension was placed into the hermetic observation chamber made of two coverslips 0.1 mm-thick separated by a gap of about 0.15 mm. All measurements were performed at room temperature (25°C).

Dual beam optical tweezers setup shown in Fig. 1 was arranged using two singlemode diode infrared lasers (Lumics LU0975M330, Germany) with wavelength of 980 nm, and output power of up to 330 mW. The diode lasers were pigtailed by polarization-maintaining optical fiber and output radiation was collimated by aspheric lenses. The position of one of the optical traps was controlled by acousto-optical deflector (Isomet LS55-NIR, USA). An oil immersion objective (Olympus UPLFLN 100XO12, Japan) with numerical aperture of 1.3, working distance of 0.2 mm and about 60% optical transmittance at 980 nm

Address all correspondence to: Andrey A. Fedyanin, Lomonosov Moscow State University, Faculty of Physics, 119991 Moscow, Russia. Tel: 0074959393910; Fax: 0074959391104; E-mail: fedyanin@nanolab.phys.msu.ru

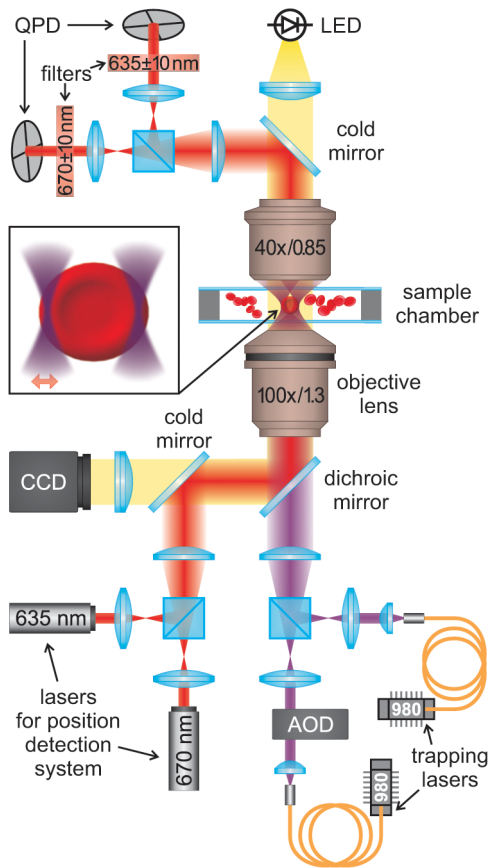


Fig. 1 Sketch of the experimental setup: double-beam optical tweezers for probing viscoelastic properties of the cells.

was used for focusing the laser beams to form the traps. Both laser beams were expanded to the full objective aperture to create maximal optical field gradient in the focal points for the most efficient RBC trapping. Two extra diode laser beams with wavelengths of 635 and 670 nm, respectively, and with the output power of 0.3 mW were used to detect displacements of the trapped cell. The latter beams passed through the optical elements controlling the positions and the width of the beams and then were focused into the sample chamber. The forward scattered light was collected by a 40X objective and detected using two quadrant photodiodes (QPDs) (Thorlabs PDQ80A, USA). Displacements of the trapped cell were extracted from the changes in the QPD photocurrent collected by analog-to-digital-converter (National Instruments PCIe-6353, USA) working at the rate of 10^5 samples per second per each channel. CCD camera was used for visual control of the trapped objects. This method is particularly sensitive for measuring displacements of the trapped spherical objects at the nanometer scale. However, the scattering pattern from the nonspherical trapped object, for example from the cell, is complex that restricts the direct measurement of displacements in the trap. Another way to quantitatively analyze the movement of the trapped cell is to measure the relative phase of the cell movement.

In the experiment single erythrocyte was doubly trapped at the edges by two independent laser tweezers with the cell being not stretched or deformed as it is schematically shown in Fig. 1. The distance between the traps was fixed to $7.5 \mu\text{m}$ while the erythrocytes studied were always selected to be of $8 \mu\text{m}$ in size. Trapping laser power in the focal plane was 20 mW per each trap

which was enough for effective cell trapping but at the same time no heating effect was observed on the time scales of the experiment duration. One of the traps was stable while the position of the second one was oscillated with an amplitude of 100 nm in the frequency range from 50 Hz to 1 kHz using acousto-optical deflector. This caused the cell vibration and the displacements of the cell edges. Position detecting lasers were also focused on the RBC edges and the scattered light was detected by QPDs.

The signal obtained by each QPD with the data acquisition time T is represented as follows:

$$\begin{aligned} f(t) &= \frac{A_0}{2} + \sum_{k=1}^{\infty} (A_k \cos k\omega_0 t + B_k \sin k\omega_0 t) \\ &= \frac{A_0}{2} + \sum_{k=1}^{\infty} C_k \sin(k\omega_0 t - \varphi_k), \end{aligned} \quad (1)$$

where

$$A_k = \frac{2}{T} \int_0^T f(t) \cos k\omega_0 t dt, \quad B_k = \frac{2}{T} \int_0^T f(t) \sin k\omega_0 t dt, \quad (2)$$

$$C_k = \sqrt{A_k^2 + B_k^2}, \quad \varphi_k = -\arctan \frac{A_k}{B_k}, \quad (3)$$

and $\omega_0 = 2\pi/T$. In the presence of external harmonical perturbation at the frequency $\omega = n\omega_0$ the phase φ_n characterizes the phase shift of the RBC edge displacement relative to the external perturbation. Provided by the cell edges displacements $f(t)_{1,2}$ the phase difference in the movement of the opposite edges of the RBC $\varphi = \varphi_{n2} - \varphi_{n1}$ and its tangent, referred to as phase difference tangent (PDT) further in the text, can be obtained using Fourier transform. The subscripts “1” and “2” refer to oscillating and fixed trap, respectively.

3 Results and Discussion

The relative phase φ of the cell edges oscillations and its tangent are measured as a function of the trap oscillation frequency ω . Figure 2 shows typical frequency dependences of the PDT. Each data set is collected during 20 s for both directions of frequency increase and decrease. The results for different directions are almost identical, therefore the time impact during the measurements is neglected and the φ values for both directions are averaged. Experimental observations showed that dependence of the PDT as a function of trap oscillation frequency is reproducibly linear one and has considerably different slopes for different types of the RBC membranes. Empty points in Fig. 2 correspond to dynamic measurements for normal living RBC. The slope value appears to be of $(-6.4 \pm 0.1) \cdot 10^{-4}$ s. Filled points represent the measurements for the RBC previously fixed by glutaraldehyde (2.5%). Glutaraldehyde solution is used as a fixative in biological applications.¹⁰ It makes the cells controllably rigid by crosslinking the proteins of the cell membrane. The slope value for glutaraldehyde-fixed RBC is equal to $(-2.7 \pm 0.2) \cdot 10^{-4}$ s.

In order to explain reproducible linear behavior of experimental dependence of the PDT upon the trap oscillations frequency the following phenomenological mechanical model shown schematically in Fig. 3 is considered. It is determined by elastic elements k and K represented by springs, which describe the trap stiffness and the RBC elastic coefficient,

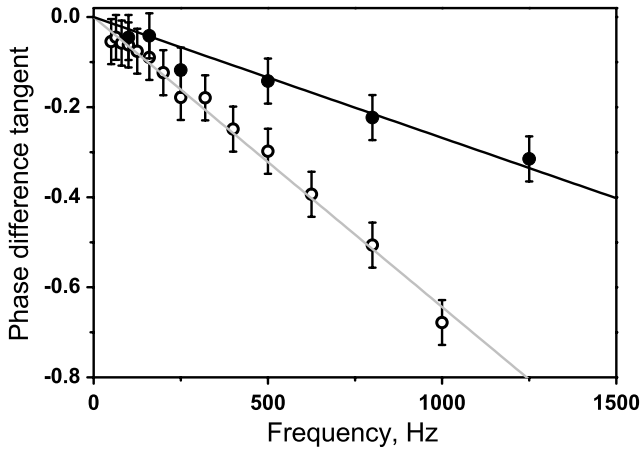


Fig. 2 Dependence of the tangent of the phase difference in the movement of the RBC edge in the fixed trap relative to the RBC edge trapped by an oscillating trap upon the frequency of the trap oscillation. Empty points correspond to the normal RBC, filled points relate to the cell fixed by glutaraldehyde (stiff membranes). Lines are linear mean-square fits to the data.

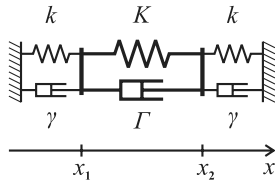


Fig. 3 Mechanical model of the trapped RBC, k is the trap stiffness, K is the RBC elastic coefficient, γ and Γ are effective viscous coefficients of the trapped system.

respectively, and by purely viscous components γ and Γ represented by dash-pots describing the effective viscous coefficients of a doubly trapped single erythrocyte. While the first trap oscillates forcing the trapped cell edge to move, the opposite cell edge faces the balance of the following viscous and elastic forces in its motion:

$$\gamma \dot{x}_2 = -k(x_2 - x_2^{\text{trap}}) + \Gamma(\dot{x}_1 - \dot{x}_2) - K(x_2 - x_1 - L), \quad (4)$$

where L is an undeformed K -spring length which is the RBC length, x_2^{trap} is a position of the second trap, x_1 and x_2 are the edges displacements from the trap centers. The variables detected in the experiment are the displacements of cell edges from the equilibrium, $y_1 = x_1 - x_1^0$, $y_2 = x_2 - x_2^0$, where $x_{1,2}^0$ are the equilibrium positions of the opposite cell edges. The second cell edge movement is then described as follows:

$$(\gamma + \Gamma)\dot{y}_2 = \Gamma\dot{y}_1 - (k + K)y_2 + Ky_1. \quad (5)$$

Let the displacement of the cell edges from equilibrium to be of $y_1 = \hat{y}_1 \exp^{i\omega t}$, $y_2 = \hat{y}_2 \exp^{i\omega t}$. Solving Eq. (5) gives:

$$(k + K + i\omega(\gamma + \Gamma))\hat{y}_2 = (K + i\omega\Gamma)\hat{y}_1. \quad (6)$$

In assumption of the frequency range $\omega^2 \ll k(k + K)/\Gamma(\Gamma + \gamma)$ the PDT is written as follows:

$$\tan \varphi = -\frac{\Gamma k - \gamma K}{k(k + K)} \omega = -\omega\tau. \quad (7)$$

The proportionality factor τ determines the viscoelastic properties of the trapped cell as a complex biological and hydrodynamical system where implementation of specific parameters is indispensable and it is impossible to pick out viscous and elastic cell properties independently. Having the dimension of time, the τ coefficient can be interpreted as an effective response time of the cell. It is related to the characteristic time of mechanical perturbation propagation in the cell. Significant change in the frequency dependence of the PDT is observed for erythrocytes with rigid membranes shown by filled points in Fig. 2. The response time τ measured for glutaraldehyde-fixed erythrocytes drastically decreases from $640 \mu\text{s}$ to $270 \mu\text{s}$ indicating considerable change in the state of the cell. This proves the ability of the offered method to detect and to control the effective rigidity of the cell.

Equation (4) is written neglecting the mass of the object studied since the case of $m\omega^2 \ll k + K$ is considered. This estimation is supported by the following experiment. In order to estimate the trap stiffness k and effective elastic parameter K for the RBC, the trapping force calibration is needed first. For this, carboxylated polystyrene $3 \mu\text{m}$ microbead (Kisker Biotech GmbH & Co. KG, PPs-3.0COOH, Germany) was connected to the RBC membrane. The bead adhered irreversibly and nonspecifically to the RBC membrane in plasma within 1 to 2 min while maintaining in contact. Then the whole system was doubly trapped by the microbead and the opposite RBC edge. The trap power for the RBC edge was set at 20 mW and the trap power for the bead varied in order to find the laser power value which would equalize the trapping force of the microbead and the RBC edge. Escape trapping forces for the bead and for the RBC edge appeared to be the same when the trap power for the bead was of $17 \pm 1 \text{ mW}$. Then, standard escape force method was used to obtain the RBC trapping force which appeared to be $29 \pm 3 \text{ pN}$. This calibration procedure is described in details in Ref. 2. Provided by the RBC escape trapping force value the trap stiffness k for the RBC edge and effective RBC elastic parameter for small deformations K was estimated by doubly trapping a single erythrocyte and by pulling one of the traps and keeping the other trap position fixed. This procedure was repeated for a numerous amount of erythrocytes and the resulted data obtained by means of optical microscopy were averaged over all the experiments. Figure 4(a) shows the dependence of the RBC edge displacement upon the RBC edge trapping force. For each data-point the maximal RBC edge displacement from its initial position in the fixed trap dx was detected before the cell slipped out from the trap. The fit of the dependence linear part gives the value of the trap stiffness to be of about $9 \text{ pN}/\mu\text{m}$. At the same time the cell elongation dl is detected for each value of the trapping force shown in Fig. 4(b). Linear fit gives the K value of about $13 \text{ pN}/\mu\text{m}$ which is of the same order as the k value. The maximal frequency value used in the experiment was 1 kHz. Since the RBC mass is about 10^{-13} kg ,¹⁸ the estimation of $m\omega^2 \ll k + K$ is reasonable for the case studied. It means that such simple mechanical model approves the experimentally obtained linear dependence of the PDT upon the trap oscillation frequency.

It is important to be aware of photo-induced effects when biological samples are exposed to laser radiation. In our case a particular care was put to estimate photodamages induced by the traps and to provide the invasiveness of the method. For this, single erythrocyte was trapped by two opposite

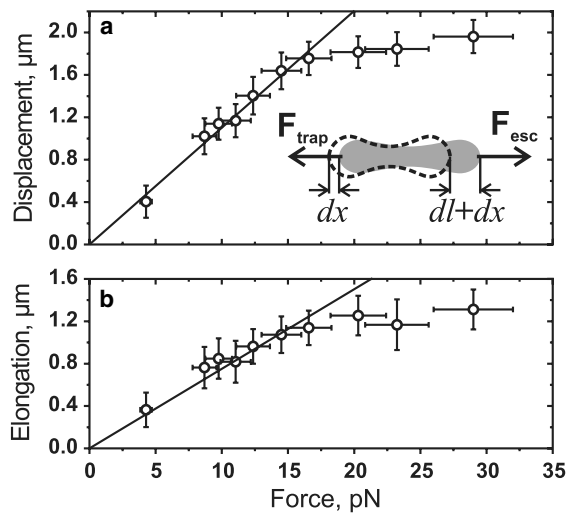


Fig. 4 (a) Dependence of the RBC edge displacement while pulling the traps apart upon the RBC edge trapping force F_{trap} . Solid line corresponds to the mean-square fit of the linear part of the data. The inset shows the schematic of the experiment, dx is the RBC edge displacement from its initial position in the fixed trap, dl is the RBC elongation. (b) Dependence of the RBC elongation upon the trapping force while stretching the cell. Solid line corresponds to the mean-square fit of the linear part of the data.

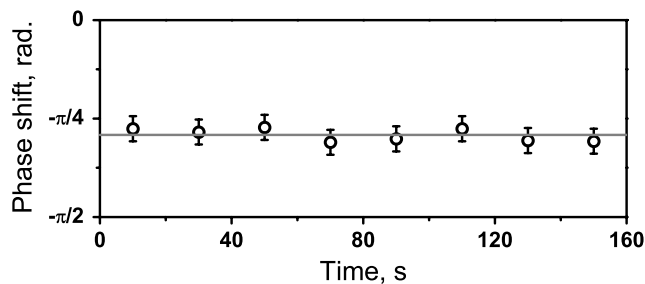


Fig. 5 Time dependence of the phase difference between oscillations of the opposite RBC edges. Frequency of the trap oscillations is 1 kHz, amplitude of the trap oscillations is 100 nm.

edges using optical tweezers. One of the traps was stable while the other one was oscillated at the frequency of 1 kHz with the amplitude of 100 nm. Displacements of the cell edges were detected as a function of experiment duration. The phase difference between oscillations of the opposite RBC edges was extracted. Time dependence of the phase difference with fixed frequency of forced oscillations shown in Fig. 5 appears to be a constant at the scales of 160 s revealing no significant change in the cell form or viscoelastic properties during the experiment. This time is long enough since typical experiment duration is about 20 s.

4 Conclusions

Double trap optical tweezers are proposed as a method for precise monitoring of red blood cells viscoelastic properties using active rheology approach combined with the forced RBC edges vibration analysis. Tangent of the phase difference obtained while the cell is doubly trapped by the fixed optical trap and the trap oscillating at the specified frequency in the range from 50 Hz to 1 kHz appears to be an effective measure of the RBC

viscoelastic properties. Phase difference tangent is found to be a reproducible linear function of the trap frequency oscillation that allows us to introduce a new effective parameter—response time—characterizing the average viscoelastic properties of an individual cell. Significant difference in the response time is obtained for normal RBCs ($640 \pm 10 \mu\text{s}$) and the cells fixed by glutaraldehyde ($270 \pm 20 \mu\text{s}$) demonstrating the sensitivity of the offered method to the living state of the cells.

Acknowledgments

This work was done using CKP facilities and was financially supported by the Russian Foundation of Basic Research and the Ministry of Education and Science of Russia. The authors gratefully acknowledge D. Kryukova for assistance in sample preparation and S. Nizamov for assistance in the development of data acquisition system.

References

1. K. C. Neuman and S. M. Block, "Optical trapping," *Rev. Sci. Instrum.* **75**(9), 2787–2809 (2004).
2. M. D. Khokhlova et al., "Normal and SLE red blood cell interactions studied by double trap optical tweezers: direct measurements of aggregation forces," *J. Biomed. Opt.* **17**(2), 025001 (2012).
3. M. Dao, C. T. Limb, and S. Suresh, "Mechanics of the human red blood cell deformed by optical tweezers," *J. Mech. Phys. Solids* **51**(11–12), 2259–2280 (2003).
4. A. Fontes et al., "Measuring electrical and mechanical properties of red blood cells with double optical tweezers," *J. Biomed. Opt.* **13**(1), 014001 (2008).
5. R. M. Hochmuth, "Micropipette aspiration of living cells," *J. Biomech.* **33**(1), 15–22 (2000).
6. E. Evans and A. A. Yeung, "Apparent viscosity and cortical tension of blood granulocytes determined by micropipet aspiration," *Biophys. J.* **56**(1), 151–160 (1989).
7. E. A. Evans, "Bending elastic modulus of red blood cell membrane derived from buckling instability in micropipet aspiration tests," *Biophys. J.* **43**(1), 27–30 (1983).
8. W. Xu, P. M. Wood-Adams, and C. G. Robertson, "Measuring local viscoelastic properties of complex materials with tapping mode atomic force microscopy," *Polymer* **47**(13), 4798–4810 (2006).
9. A. B. Mathur et al., "Endothelial, cardiac muscle and skeletal muscle exhibit different viscous and elastic properties as determined by atomic force microscopy," *J. Biomech.* **34**(12), 1545–1553 (2001).
10. M. P. M. Marinkovic et al., "Viscoelasticity of the human red blood cell," *Am. J. Physiol., Cell Physiol.* **293**(2), C597–C605 (2007).
11. K. Dholakia and T. Cizmar, "Shaping the future of manipulation," *Nat. Photon.* **5**(6), 335–342 (2011).
12. F. M. Fazal and S. M. Block, "Optical tweezers study life under tension," *Nat. Photon.* **5**(6), 318–321 (2011).
13. A. G. Zhdanov et al., "Detection of plasmon-enhanced luminescence fields from an optically manipulated pair of partially metal covered dielectric spheres," *Opt. Lett.* **33**(23), 2749–2751 (2008).
14. J. P. Mills et al., "Nonlinear elastic and viscoelastic deformation of the human red blood cell with optical tweezers," *Mech. Chem. Biosyst.* **1**(3), 169–180 (2004).
15. G. Lenormand et al., "Direct measurement of the area expansion and shear moduli of the human red blood cell membrane skeleton," *Biophys. J.* **81**(1), 43–56 (2001).
16. D. Mizuno et al., "Nonequilibrium mechanics of active cytoskeletal networks," *Science* **315**(5810), 370–373 (2007).
17. J. C. Meiners and S. R. Quake, "Direct measurement of hydrodynamic cross correlations between two particles in an external potential," *Phys. Rev. Lett.* **82**(10), 2211–2214 (1999).
18. Y. Hashimoto et al., "Erythrocyte mean cell volume and genetic polymorphism of aldehyde dehydrogenase 2 in alcohol drinkers," *Blood* **99**(9), 3487–3488 (2002).